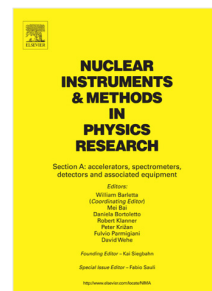


Journal Pre-proof

Measurement of the energy of fast neutrons in the presence of gamma rays using a NaI(Tl) and a plastic scintillator

Xiaobing Li, Zhonghai Wang, Huanwen Lv, Shuping Wei, Jiajia Liu, Yudong Wang, Xing Fan, Rong Zhou, Chaowen Yang



PII: S0168-9002(20)30653-7
DOI: <https://doi.org/10.1016/j.nima.2020.164257>
Reference: NIMA 164257

To appear in: *Nuclear Inst. and Methods in Physics Research, A*

Received date: 22 April 2020
Revised date: 5 June 2020
Accepted date: 6 June 2020

Please cite this article as: X. Li, Z. Wang, H. Lv et al., Measurement of the energy of fast neutrons in the presence of gamma rays using a NaI(Tl) and a plastic scintillator, *Nuclear Inst. and Methods in Physics Research, A* (2020), doi: <https://doi.org/10.1016/j.nima.2020.164257>.

This is a PDF file of an article that has undergone enhancements after acceptance, such as the addition of a cover page and metadata, and formatting for readability, but it is not yet the definitive version of record. This version will undergo additional copyediting, typesetting and review before it is published in its final form, but we are providing this version to give early visibility of the article. Please note that, during the production process, errors may be discovered which could affect the content, and all legal disclaimers that apply to the journal pertain.

© 2020 Published by Elsevier B.V.

1 **Measurement of the energy of fast neutrons in the presence of gamma**
2 **rays using a NaI(Tl) and a plastic scintillator**

3 Xiaobing Li^a, Zhonghai Wang^{a,*}, Huanwen Lv^b, Shuping Wei^b, Jiajia Liu^b, Yudong
4 Wang^a, Xing Fan^b, Rong Zhou^a, Chaowen Yang^a

5 ^aCollege of Physics, Key Laboratory of Radiation Physics and Technology, Ministry of Education, Sichuan University,
6 Chengdu, 610064, China

7 ^bNuclear Power Institute of China, Chengdu, 610213, China

8 *Corresponding author, Email address: zhonghaiwang@scu.edu.cn

9

10 A B S T R A C T

11 In many radiological laboratories, the energies of fast neutrons are very important for
12 radiation diagnostics. In this paper we propose a method based on NaI and plastic
13 scintillation (PS) detectors that measures the fast neutrons. The PS detector is sensitive
14 to both gamma rays and fast neutrons. The NaI(Tl) detector is only sensitive to gamma
15 rays. By subtracting the gamma information from the neutron–gamma mixed energy
16 spectrum, pure neutron radiation information is obtained. Then, applying an unfolding
17 method, the energy distribution of the fast neutron is generated. To verify this method,
18 an experiment measuring the energy of monoenergetic neutrons was performed with
19 the result confirming the effectiveness of this method.

20 *Keywords:*

21 Fast neutron detection; NaI(Tl) scintillation detector; Plastic scintillation detector;
22 Gravel algorithm.

23

24 **1. Introduction**

25 The measurement of fast-neutron energies is an important procedure in radiation
26 monitoring and diagnostics. With the wide use of neutron detection technology in many
27 fields such as nuclear physics research, nuclear technology applications, and radiation
28 protection, fast-neutron energy is a key physical quantity^{14[1]}. There are two main
29 difficulties associated with this procedure: as the neutron is not electrically charged, the
30 measurement must involve inherently the neutron reaction products; moreover, neutron
31 and gamma rays often coexist, so the influence of gamma rays must be considered^{12[3]}.

32 In the last decade, neutron detection technology has advanced, although extracting the
33 energy spectrum of neutron radiation remains a challenge.

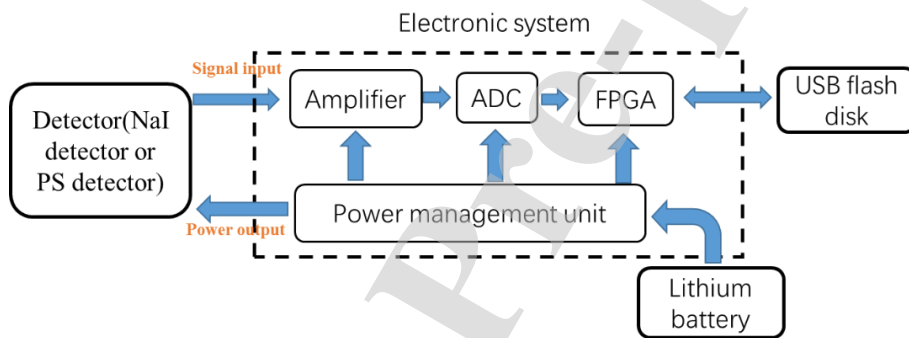
34 Common devices used in neutron-energy measurements include Bonner spheres^[4]
35 and organic scintillation detectors^[5]. Bonner spheres normally include tens of
36 polyethylene spheres of different diameters usually ranging from 2 inches to 12
37 inches^{[6][7]}. **Because of the larger numbers and the size of polyethylene spheres, the
38 Bonner spheres usually takes up a large space and are complicated to use and unsuitable
39 in some small narrow spaces.** Organic scintillators usually refer to either liquid or
40 plastic scintillators. Both fast neutrons and gamma rays are detected by organic
41 scintillators. Therefore, pulse-shape discrimination (PSD) of neutron and γ -rays is
42 performed when using organic scintillators for detecting fast neutrons. The PSD needs
43 a special scintillator to achieve the objective. Additionally, being both inflammable and
44 toxic, the liquid scintillator is not able to be used in some workplaces. **Recently the PSD
45 has been applied in plastic scintillation detector successfully. However, PSD techniques
46 usually need more complex electronics than multi-channel, which is more susceptible
47 to environmental impact. And in some workplaces such as reactors, where the
48 environment is complex and the ambient temperature is changing, the PSD method may
49 fail.**

50 In this paper, we propose a different method based on a NaI(Tl) scintillation detector
51 and a plastic scintillation (PS) detector to measure the energy spectra of fast neutrons.
52 First, the gamma energy spectrum is measured with the NaI(Tl) scintillation detector.
53 At the same time, the mixed energy deposition spectrum of gamma rays and neutrons
54 is measured using the PS detector. The second step involves calculating the incident
55 gamma-ray spectrum by unfolding the gamma-ray spectrum obtained by the NaI
56 detector and computing the gamma-ray pulse-height spectrum of the PS detector. The
57 next step involves extracting the gamma ray part from the mixed energy deposition
58 spectrum to arrive at the pure neutron deposition spectrum. Lastly, by unfolding the
59 neutron deposition spectrum using the Gravel algorithm, the neutron energy spectrum
60 is produced.

61 2. Method and materials

62 2.1. Detection system

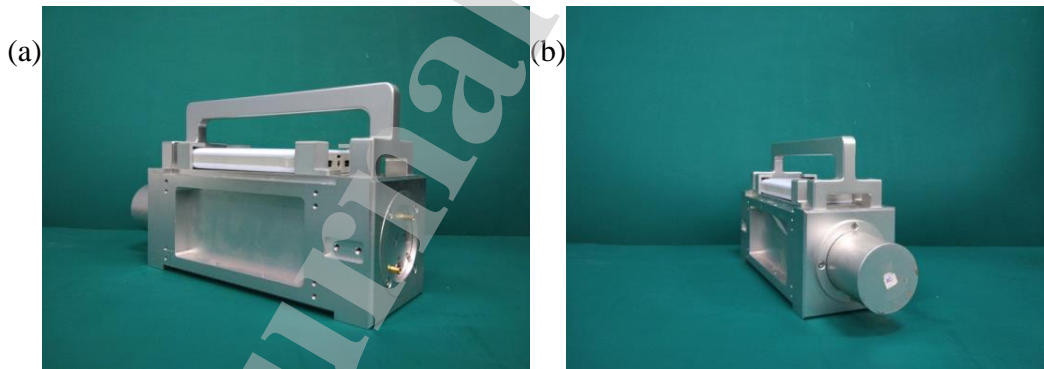
63 The detection system includes a NaI(Tl) detector, a PS detector, and the electronics
 64 system. The NaI(Tl) detector (Model CH281, HAMAMATSU Corp, Japan) has a
 65 NaI(Tl) scintillator that is cylindrical in shape of dimension $\Phi 50 \times 50$ mm. Similarly, the
 66 PS detector (EJ 299-33A, Eljen Technology, Sweetwater, TX) has a cylindrical
 67 scintillator of the same size. The electronic systems for these independently-designed
 68 detectors include amplifier, ADC, FPGA, and a power management unit. A schematic
 69 of the electronics is shown in Fig. 1. To protect the scintillator and circuit, and for ease
 70 in transporting, a metal shell was especially designed for the whole detection device
 71 (Fig. 2).



72

73

Fig. 1. Electronic block diagram of detection system.



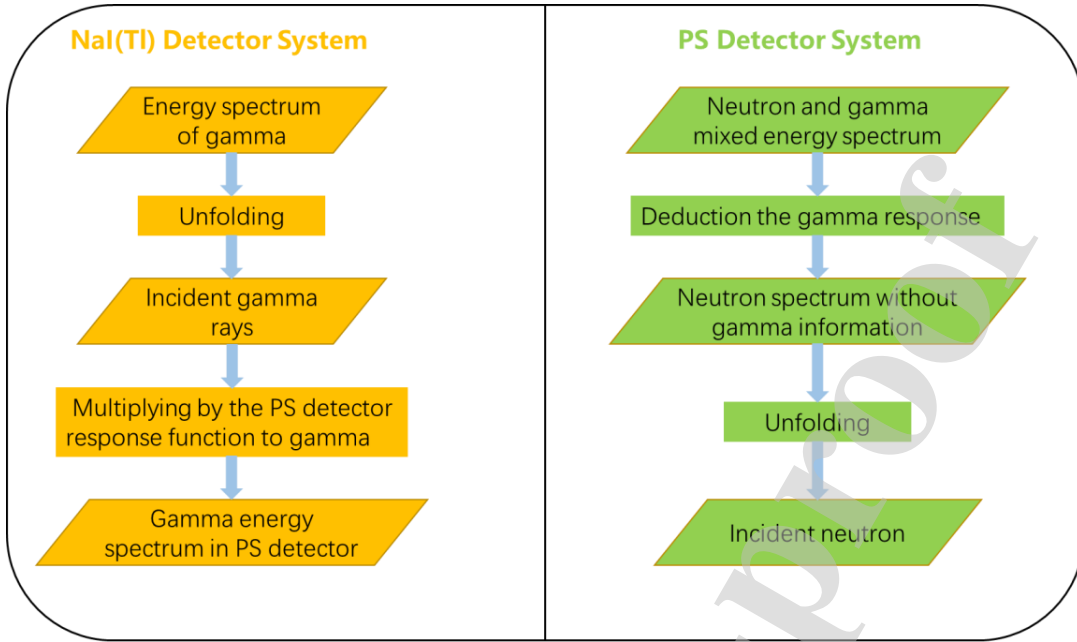
74

Fig. 2. Actual detection system: (a) PS detection system; (b) NaI(Tl) scintillation detection system.

76 2.2. Method

77 In the method (Fig. 3), two types of scintillation detectors, NaI(Tl) and plastic,
 78 were used. The NaI(Tl) scintillator has a very small neutron reaction cross, and hence
 79 seldom interacts with fast neutrons. The pulse-height spectrum obtained from NaI(Tl)
 80 almost only contains gamma-ray information. The plastic scintillator can detect

81 simultaneously fast neutrons and gamma rays.



82
83 **Fig. 3.** Flow chart of the method

84 With the NaI detector being only sensitive to gamma rays, the incident gamma-ray
85 energy is determined by unfolding the pulse-height spectra detected by the NaI(Tl)
86 detector. Then, multiplying the incident gamma energy by the response function of the
87 PS detector to gamma rays yields the energy deposition spectrum of incident gamma
88 rays in the PS detector. Next, the gamma pulse-height spectrum is subtracted from the
89 mixed energy deposition spectrum to obtain the neutron energy deposition spectrum.
90 Finally, unfolding the neutron energy spectrum, the incident neutron energy is obtained.

91 2.2.1. Unfolding method

92 The unfolding procedure includes unfolding gamma rays and neutron.
93 Mathematically, both are the same and use the same algorithm. The response of the
94 scintillation detector to gamma rays or neutron is described using the response matrix
95 R . The pulse height spectrum (PHS) of the differential energy spectrum $\Phi_E(E)$ is
96 described by the linear equation^[8]

$$97 \quad N_i = \int R_i(E) \Phi_E(E) dE, \quad (1)$$

98 where N_i is the number of counts in channel i of the PHS ($i=1, \dots, n$, n being the number
99 of channels), and $R_i(E)$ the scintillation detector response of channel i to a particle of
100 energy E . Equation (1) is convenient as N_i reduces to the discrete form ready for

101 computation,

$$102 \quad N_i = \sum_j R_{ij} \Phi_j, \quad (2)$$

103 where R_{ij} is the element of the response matrix and Φ_j is the j -th component of the
104 fluence vector ($j=1, \dots, m$, and m being the number of bins used in partitioning the energy
105 of the incident gamma rays or neutrons).

106 The objective in the unfolding procedure is to determine the unknown Φ from the
107 measured N_i and response R . To solve this problem, there are several mathematical
108 methods including least-squares^[9], Monte Carlo method^[10], maximum entropy
109 method^[11], genetic algorithm^[12], and artificial neural networks^{[13][14]}. The commonly
110 used and most developed codes for unfolding include SAND-II^[15], Gravel^[16], and
111 UMG^[17].

112 The Gravel method is an iterative unfolding algorithm, and has been successfully
113 used for unfolding gamma-ray spectra^[18]. Recently this method was used to unfold a
114 fast neutron spectrum measured by a scintillation detector^[19]. In the present method,
115 the Gravel algorithm is used to unfold both neutron and gamma-ray spectra. In brief,
116 the Gravel algorithm is^{[19][20]}

$$117 \quad \Phi_j^{K+1} = \Phi_j^K \exp \left(\frac{\sum_i W_{ij}^K \ln \left(\frac{N_i}{\sum_{j'} R_{ij'} \Phi_{j'}^K} \right)}{\sum_i W_{ij}^K} \right), \quad (3)$$

118 where W_{ij}^K is called the weight factor, defined by

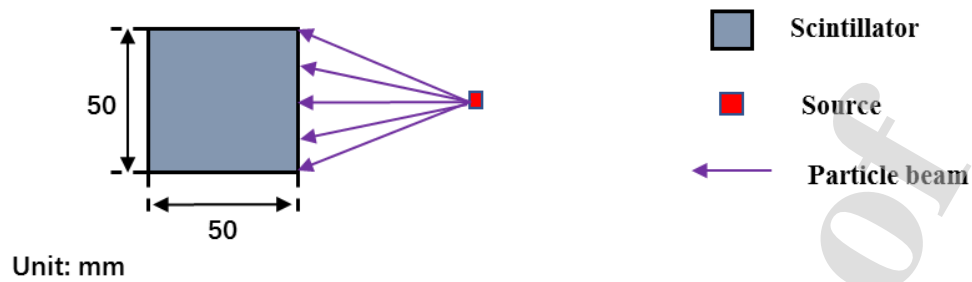
$$119 \quad W_{ij}^K = \frac{R_{ij} \Phi_j^K}{\sum_{j'} R_{ij'} \Phi_{j'}^K} \cdot \frac{N_i^2}{\sigma_i^2}, \quad (4)$$

120 where σ_i^2 is the estimate of the measurement error, and K is the number of iterations.

121 2.2.2. Response function

122 To apply this algorithm to the detection system, the response matrices of the
123 NaI(Tl) detector to incident gamma rays and of the PS detector to incident gamma rays
124 and neutrons must be determined. In this study, the response matrices were calculated
125 using the Geant4 code. **In the simulation, two scintillators, one is NaI scintillator, the
126 shape of dimension of which is $\Phi 50 \times 50$ mm, the other PS scintillator with the same
127 size, were modeled in the Monte Carlo code.** The simulation model is shown in Fig. 4.

128 The outer side of the crystal is wrapped with a layer of aluminum sheet with a thickness
 129 of 1 mm to protect the scintillators.



130

131

Fig. 4. The simulation model.

132

133

134

135

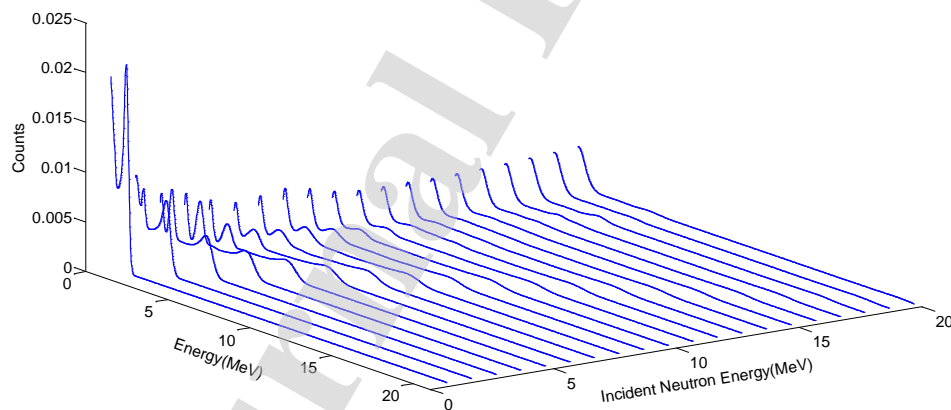
136

137

138

139

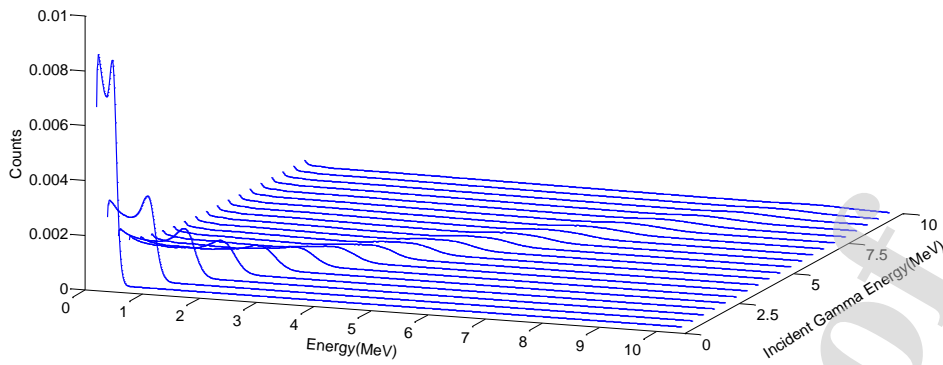
In the simulation the radioactive source is located directly in front of the crystal and the emission angle of rays is randomly from 0 degrees to 360 degrees. There is air at room temperature between the detector and the radioactive source. The range of response for the PS detector to neutrons is from 20 keV to 20.48 MeV; the energy spacing chosen was 20 keV. The response function is plotted in Fig. 5. The response functions of the PS and NaI(Tl) detector to gamma rays are shown in Figs. 6 and 7, both having the same energy range from 10 keV to 10.24 MeV, with the energy spacing set at 10 keV.



140

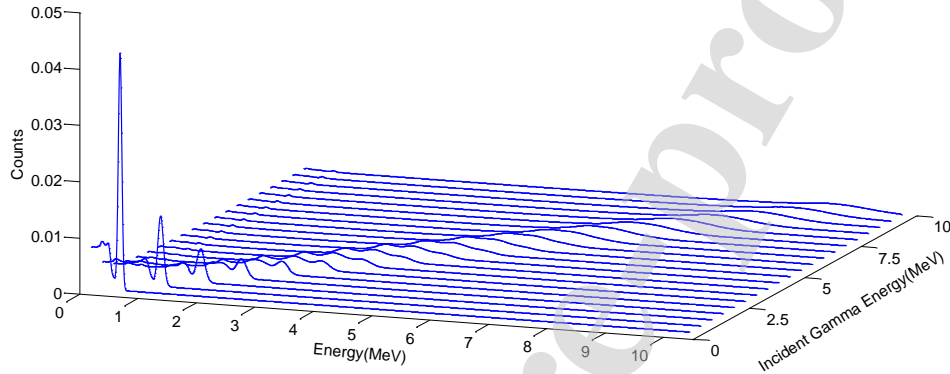
141

Fig. 5. Response function of the EJ299-33 scintillator to neutrons



142
143

Fig. 6. Response function of the PS detector to gamma rays.



144
145

Fig. 7. Response function of the NaI(Tl) detector to gamma rays

146 **3. Experiment and results**

147 Using this method, an experiment to detect the energy spectrum of monoenergetic
148 neutrons was carried out at the Accelerator Laboratory, Institute of Nuclear Science and
149 Technology, Sichuan University. By comparing the experimental results with the
150 theoretical neutron energies, we verified the performance of the method proposed.

151 *3.1. Calibration*

152 Before the experiment, the calibration for the both detector was carried on. The
153 NaI(Tl) scintillation detector, which is used to detect gamma rays, was calibrated
154 directly with a γ radioactive source. In this study, ^{22}Na and ^{137}Cs sources were used for
155 the calibration. The calibration resulted in the correlation

$$156 \quad E_{\gamma} = 13.14 \times ch - 113, \quad (5)$$

157 where E_{γ} denotes the energy of the gamma rays, the unit being keV; ch is the number
158 of the channel.

159 The PS detector is used for detecting gamma rays and neutrons. The constituents
160 of the PS are low atomic number elements such as hydrogen and carbon, so the main

161 reaction type is Compton scattering of gamma rays. The pulse-height spectrum obtained
 162 from the PS detector is different from that obtained from an inorganic scintillation
 163 detector; indeed, the full energy peak is ‘missing’^[21]. To calibrate the PS detector, we
 164 combined Monte Carlo simulation results and experimental results. Details of the
 165 method can be found in Ref. [21]. Similar to Eq. (5), the calibration result establishes
 166 the correlation,

$$167 \quad E_{\gamma} = 1.631 \times ch + 34.1. \quad (6)$$

168 The PS detector is sensitive to fast neutrons. The most important reaction
 169 undertaken by fast neutrons in the plastic scintillator is elastic scattering producing
 170 mainly a hydrogen recoil. The maximum energy in the hydrogen recoil is equal to the
 171 energy of the incident neutron. With the PS detector calibrated for gamma rays, the
 172 energy corresponds to the energy deposition in the electrons of the scintillator. For fast
 173 neutrons, it is the recoil hydrogen that loses energy in the scintillator. To calculate the
 174 recoiling protons energy, a correlation between electron-equivalent energy and the
 175 recoiling protons energy must be determined. The correlation for the type of PS detector
 176 used was deduced by Nyibule and Henry^[22], specifically,

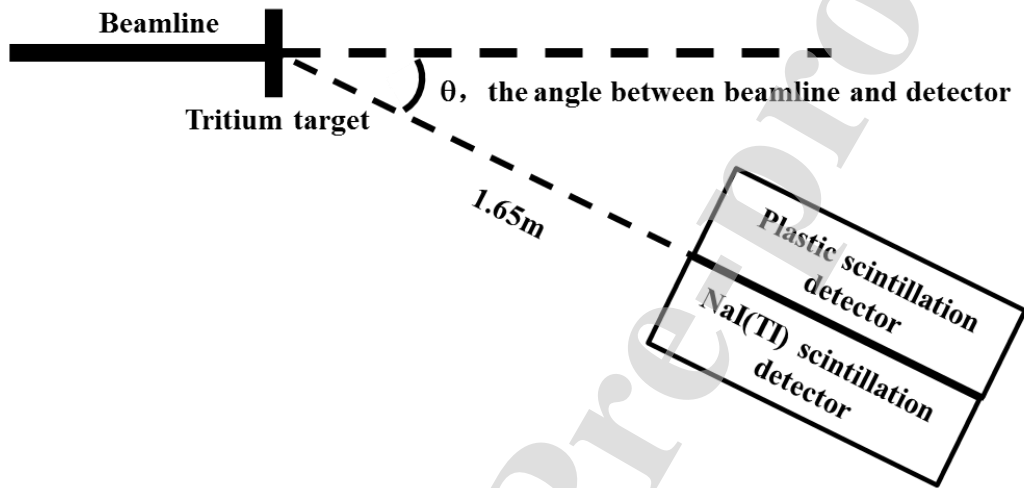
$$177 \quad L = -0.15 + 0.25 \times E_{rp} + 0.0096 \times E_{rp}^2, \quad (7)$$

178 where E_{rp} denotes the energy of the recoiling protons, the unit being MeV; L is the light
 179 output function, its units being the electron-equivalent MeV, namely, MeVee.

180 3.2. Experiment and results

181 Various nuclear reactions emit neutrons including D(d,n), T(d,n), and T(p,n)
 182 reaction. In the experiment, we chose the T(d,n) reaction. A deuterium beam was
 183 generated at the accelerator and directed onto a tritium target. The target is solid tritium-
 184 titanium (T-Ti) target, which has a thickness of 1.833 mg/cm², and the atom ratio of T
 185 to Ti is 1.84. Tantalum foil is behind the tritium-titanium target which could stop the
 186 proton beam. At the end of the target, a continuous cooling water flow with a thickness
 187 of 4 mm was used to avoid local overheating^[23]. In the experimental setup (Fig. 8), the
 188 detector and tritium target were in the same horizontal plane, their separation being 1.65
 189 m. Because of the experimental conditions, the deuterium beam was accelerated to 1.5

190 MeV. The available angles between the beamline and detector were 30°, 60°, and 90°
 191 yielding corresponding neutron energies of 17.14 MeV, 16.04 MeV, and 14.64 MeV.
 192 The experimental setup (Fig. 9) has the PS detector and NaI(Tl) scintillation detector
 193 fixed on a red metal support facing the target. **In the experiment the distance between**
 194 **target is about 1.65 m and the distance for the two probes of the detectors is about 10.5**
 195 **cm, so the largest angle gap for the two detectors is about 1.8°. With the subtle gap the**
 196 **different angles hardly affect the experimental results.**



197
 198

Fig. 8. Schematic of the geometry of the experimental setup.

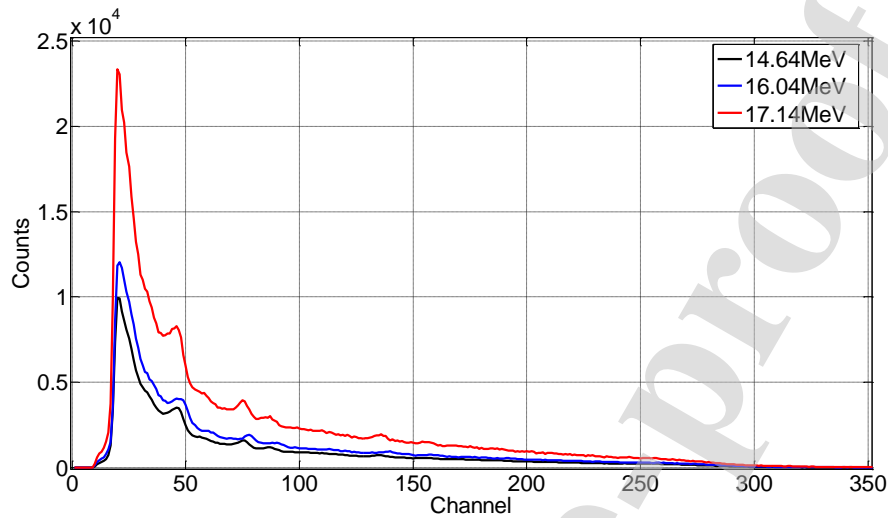


199
 200
 201

Fig. 9. Photograph of the experimental setup.

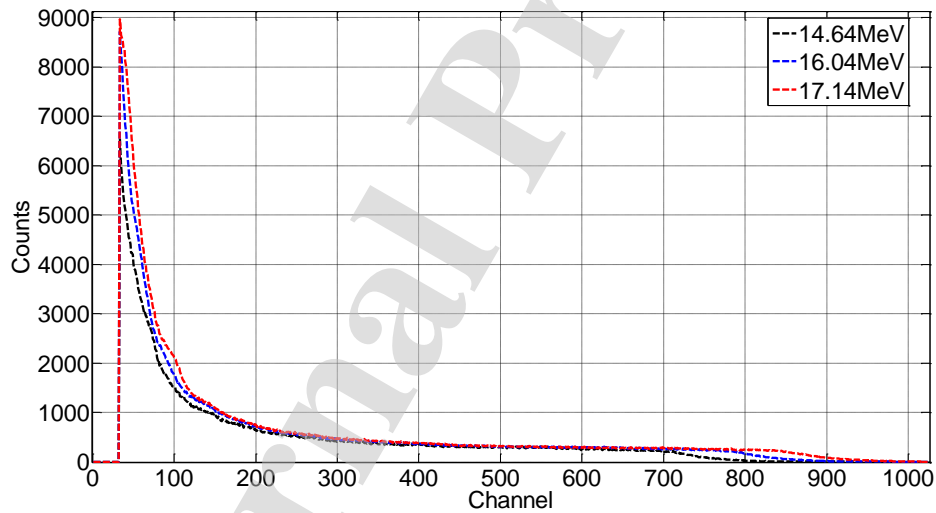
The experimental results (Fig. 10, Fig. 11) include the detection data of the PS and

202 NaI detectors. The deduction and unfolding results are demonstrated in Fig. 12, Fig. 13
 203 and Fig. 14. Given the incident neutron energies of 14.64 MeV, 16.04 MeV, and 17.14
 204 MeV, the corresponding peaks of the unfolded incident neutron spectra are 15.03 MeV,
 205 16.36 MeV, and 16.67 MeV, respectively.



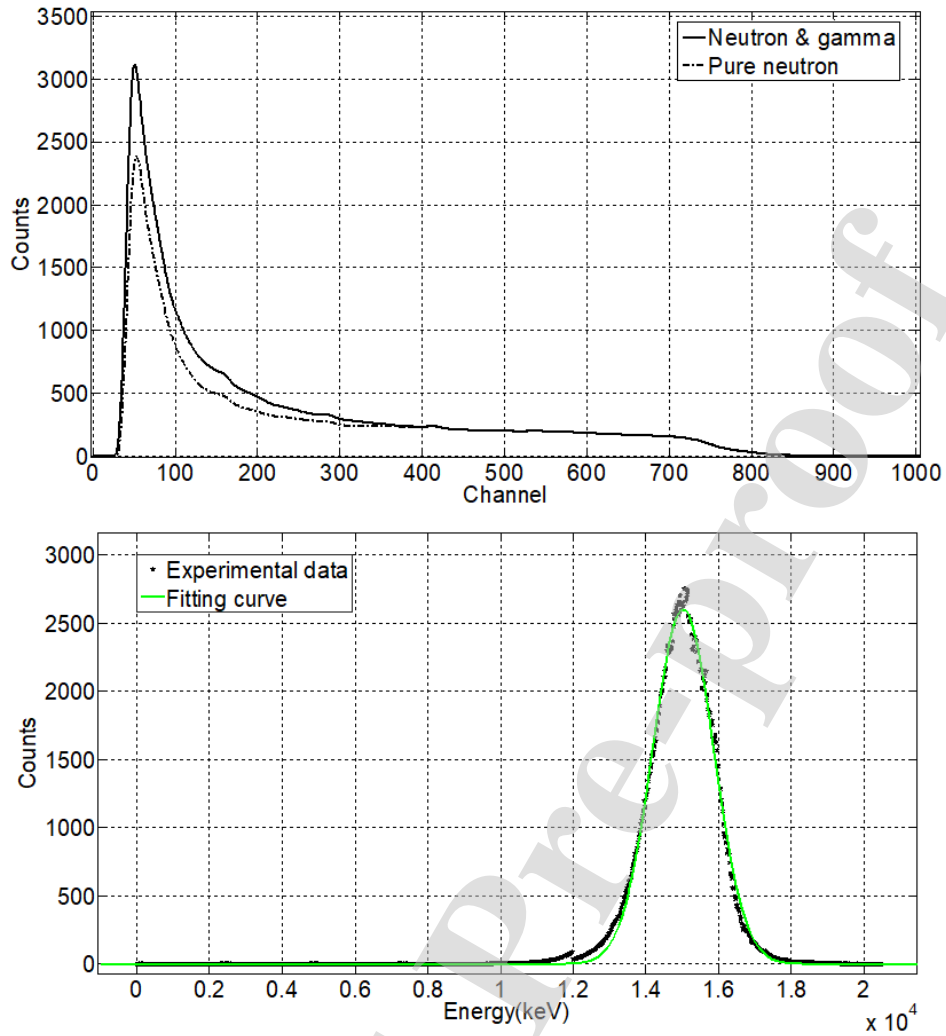
206
 207
 208

Fig. 10. Pulse-height spectrum detected by NaI detector when the energies of the neutron are 14.64 MeV, 16.04 MeV, and 17.14 MeV.



209
 210
 211

Fig. 11. Pulse-height spectrum detected by PS detector when the energies of the neutron are 14.64 MeV, 16.04 MeV, and 17.14 MeV.



212

213

214

215

216

Fig. 12. The results of deduction and the unfolded incident energy spectrum of 14.64 MeV neutron. The upper picture shows the pure neutron spectrum and the gamma-neutron mixed spectrum in PS detector. The picture below shows the calculating neutron energy distribution and the result of fitting data with Gaussian function.

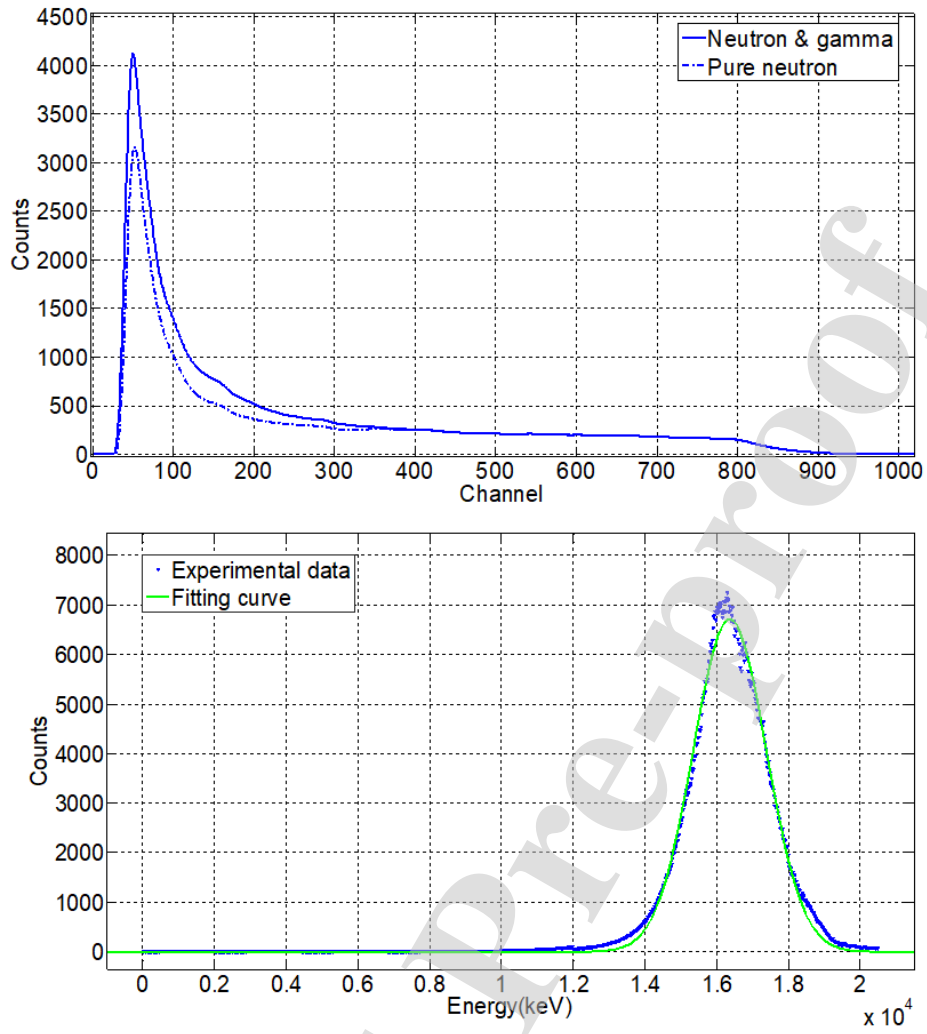
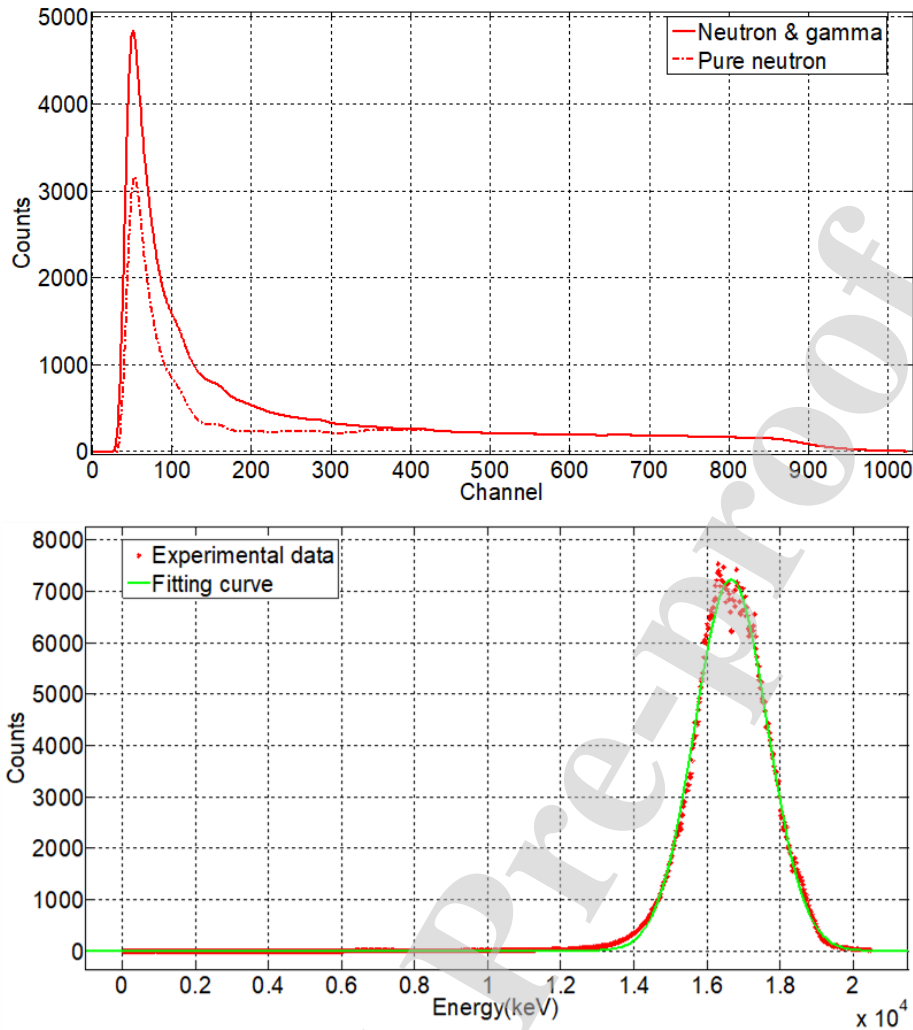


Fig. 13. The results of deduction and the unfolded incident energy spectrum of 16.04 MeV neutron.

217
218
219
220



221
 222 **Fig. 14.** The results of deduction and the unfolded incident energy spectrum of 17.14 MeV
 223 neutron.

224 These spectra demonstrate that for all three incident mono-energy neutron beams,
 225 the neutron energy can be calculated using this spectral method. These incident neutron
 226 spectra only include one peak and the peak position is close to the theoretical values.
 227 Thus, the experimental results are consistent with theoretical predictions. From the
 228 unfolding results it can be also seen that there is an obvious broaden of the neutron
 229 energy. First the statistical fluctuation of data is inevitable. Second there are a lot of
 230 scattering even during the whole experiment, which adds the straggling of neutron
 231 energy. The unfolding algorithm is a kind of iterative algorithms and the computing
 232 results has acceptable error. The response function is computed by simulation, which is
 233 different with the real response, and this increases the unfolding error. Last the two
 234 detector have intrinsic resolution. All the factors mentioned are contributed to the width

235 of the peaks.

236 4. Conclusion

237 We proposed a method to obtain the energy spectra of fast neutrons that employed
238 both a PS (plastic scintillation) and a NaI(Tl) scintillation detector. The experimental
239 results show that the method is reliable. There is still a disparity between experimental
240 and theoretical neutron energies. When calibrating these detectors, ^{22}Na and ^{137}Cs were
241 used. The two radioactive sources emit low energy γ rays, below 2 MeV thereby
242 incurring a calibration error in the high energy range. For gamma rays, both detectors
243 have different lower limits, which lead to errors in the deduction procedure at low
244 energies.

245 Because of limitations in the experimental conditions, only three energy points
246 were used to verify the method, the energy range being 14–17 MeV. Under current
247 experimental conditions, the energy of the available gamma-ray source is below 2 MeV.
248 We plan to verify the method with monoenergetic neutron of different energies that
249 extend the present range of energies and modify the calibration parameters with the
250 gamma-ray source with energies over 2 MeV. Considering the method is feasible to use
251 and the gamma information can be known by the NaI detector, it provides new
252 opportunities in the field of neutron detection.

253 Acknowledgments

254 This work was supported by the Sichuan Province Key Research and Development
255 Program (No.2018GZ0524), National Natural Science Foundation of China (Grant No.
256 U1967205), the Postdoctoral Fund of Sichuan University (No.20826041C4158).
257 Thanks to Xiaobing Luo of Institute of Nuclear Science and Technology, Sichuan
258 University and Bowen Zheng of School of Physical Science, University of Science and
259 Technology of China for their help in the experiment.

260 Reference

- 261 [1] D.J. Thomas, A. V. Alevra, Bonner sphere spectrometers - A critical review, Nucl. Instruments
262 Methods Phys. Res. Sect. A Accel. Spectrometers, Detect. Assoc. Equip. 476 (2002) 12–20.
263 doi:10.1016/S0168-9002(01)01379-1.
- 264 [2] J. Iwanowska, L. Swiderski, M. Moszynski, T. Szczesniak, P. Sibczynski, Z. Galunov, L.

- 265 Karavaeva, Neutron/gamma discrimination properties of composite scintillation detectors, J.
266 Instrum. 6 (2011). doi:10.1088/1748-0221/6/07/P07007.
- 267 [3] J. Iwanowska, T. Szcz, *New Organic Scintillators for Neutron Detection*, Aip Conference
268 American Institute of Physics. 165 (2010) 1–4. doi:10.1063/1.3295632.
- 269 [4] G.F. Knoll, *Radiation detection and measurement / Glenn F. Knoll. Radiation detection and*
270 *measurement. Wiley, 1989.*
- 271 [5] R.L. Bramblett, R.I. Ewing, T.W. Bonner, A new type of neutron spectrometer ☆, Nucl.
272 Instruments Methods. 9 (1960) 1–12.
- 273 [6] M.E. Toms, A computer analysis to obtain neutron spectra from an organic scintillator, Nucl.
274 Instruments Methods. 92 (1971) 61–70.
- 275 [7] V. Lacoste, V. Gressier, J.L. Pochat, F. Fernández, M. Bakali, T. Bouassoule, Characterization of
276 Bonner sphere systems at monoenergetic and thermal neutron fields, Radiat. Prot. Dosimetry. 110
277 (2004) 529–532. doi:10.1093/rpd/nch279.
- 278 [8] M. Reginatto, Overview of spectral unfolding techniques and uncertainty estimation, Radiat.
279 Meas. 45 (2010) 1323–1329. doi:10.1016/j.radmeas.2010.06.016.
- 280 [9] R. Koochi-Fayegh, S. Green, M.C. Scott, Comparison of neutron spectrum unfolding codes used
281 with a miniature NE213 detector, Nucl. Instruments Methods Phys. Res. Sect. A Accel.
282 Spectrometers, Detect. Assoc. Equip. 460 (2001) 391–400. doi:10.1016/S0168-9002(00)01069-X.
- 283 [10] R. Sanna, O. Brien, *MONTE-CARLO UNFOLDING OF NEUTRON SPECTRA*, Nuclear
284 *Instruments & Methods* 91 (1971) 573–576.
- 285 [11] M. Reginatto, P. Goldhagen, S. Neumann, Spectrum unfolding, sensitivity analysis and
286 propagation of uncertainties with the maximum entropy deconvolution code MAXED, Nucl.
287 Instruments Methods Phys. Res. Sect. A Accel. Spectrometers, Detect. Assoc. Equip. 476 (2002)
288 242–246. doi:10.1016/S0168-9002(01)01439-5.
- 289 [12] B. Mukherjee, BOND1-97: a novel neutron energy spectrum unfolding tool using a genetic
290 algorithm, Nucl. Instruments Methods Phys. Res. Sect. A Accel. Spectrometers, Detect. Assoc.
291 Equip. 432 (1999) 305–312. doi:10.1016/S0168-9002(99)00535-5.
- 292 [13] H.R. Vega-Carrillo, V. Martín Hernández-Dávila, E. Manzanares-Acuña, G.A.M. Sánchez, M.P.I.
293 De La Torre, R. Barquero, F. Palacios, R.M. Villafañe, T.A. Arteaga, J.M.O. Rodriguez, Neutron
294 spectrometry using artificial neural networks, Radiat. Meas. 41 (2006) 425–431.

- 295 doi:10.1016/j.radmeas.2005.10.003.
- 296 [14] S. Avdic, S.A. Pozzi, V. Protopopescu, Detector response unfolding using artificial neural
297 networks, Nucl. Instruments Methods Phys. Res. Sect. A Accel. Spectrometers, Detect. Assoc.
298 Equip. 565 (2006) 742–752. doi:10.1016/j.nima.2006.06.023
- 299 [15] P.J. Griffin, J.G. Kelly, J.W. Vandenburg, User 's Manual for SNL-SAND-II Code, Sandia Rep.
300 Sand93-3957. (1994) 104.
- 301 [16] M. Matzke, *The HEPROW Program System*, Physikalisch-Technische Bundesanstalt (2003).
- 302 [17] N.J. Roberts, Investigation of combined unfolding of neutron spectra using the UMG unfolding
303 codes, Radiat. Prot. Dosimetry. 126 (2007) 398–403. doi:10.1093/rpd/ncm082.
- 304 [18] K. Kudo, N. Takeda, S. Koshikawa, H. Toyokawa, H. Ohgaki, M. Matzke, Photon spectrometry
305 in thermal neutron standard field, Nucl. Instruments Methods Phys. Res. Sect. A Accel.
306 Spectrometers, Detect. Assoc. Equip. 476 (2002) 213–217. doi:10.1016/S0168-9002(01)01434-6.
- 307 [19] Y.H. Chen, X.M. Chen, J.R. Lei, L. An, X.D. Zhang, J.X. Shao, P. Zheng, X.H. Wang, Unfolding
308 the fast neutron spectra of a BC501A liquid scintillation detector using GRAVEL method, Sci.
309 China Physics, Mech. Astron. 57 (2014) 1885–1890. doi:10.1007/s11433-014-5553-7.
- 310 [20] M. Matzke, Unfolding of Particle Spectra Manfred Matzke Physikalisch-Technische
311 Bundesanstalt (PTh), D-381 16 Braunschweig, Germany, 2867 (n.d.) 598–607.
- 312 [21] X. Li, Y. Wang, R. Zhou, C. Yan, Energy calibration for plastic scintillation detectors based on
313 Compton scatterings of gamma rays, J. Instrum. 12 (2017) P12025–P12025.
- 314 [22] S. Nyibule, E. Henry, Radioluminescent characteristics of the EJ 299-33 plastic scintillator, Nucl.
315 Instruments Methods Phys. Res. Sect. A Accel. Spectrometers, Detect. Assoc. Equip. 728 (2013)
316 36–39. doi:10.1016/j.nima.2013.06.020.
- 317 [23] Su Shen, Zhiling Yuan, Xiaobing Luo, Measurement of ^{232}Th neutron capture cross-sections in
318 the energy range of 2.0–5.0 MeV by using the neutron activation technique, Nucl. Instruments
319 Methods Phys. Res. Sect. B. 476 (2020) 59–63. doi: 10.1016/j.nimb.2020.04.028.
- 320

Credit author statement

XiaoBing Li: Conceptualization, Methodology, Writing - Original Draft, Writing - Review & Editing.

Zhonghai Wang: Conceptualization, Project administration.

Huanwen Lv: Funding acquisition.

Shuping Wei: Software.

Jiajia Liu: Investigation.

Yudong Wang: Formal analysis.

Xing Fan: Data Curation.

Rong Zhou: Supervision.

Chaowen Yang: Resources.

Declaration of interests

The authors declare that they have no known competing financial interests or personal relationships that could have appeared to influence the work reported in this paper.

The authors declare the following financial interests/personal relationships which may be considered as potential competing interests:

Journal Pre-proof